Inorganic Chemistry

Article

pubs.acs.org/IC

Redox-Active Porous Coordination Polymers Prepared by Trinuclear Heterometallic Pivalate Linking with the Redox-Active Nickel(II) Complex: Synthesis, Structure, Magnetic and Redox Properties, and Electrocatalytic Activity in Organic Compound Dehalogenation in Heterogeneous Medium

A. S. Lytvynenko,[†] S. V. Kolotilov,*[,†] M. A. Kiskin,[‡] O. Cador,[§] S. Golhen,[§] G. G. Aleksandrov,[‡] A. M. Mishura,[†] V. E. Titov,[†] L. Ouahab,[§] I. L. Eremenko,*[,‡] and V. M. Novotortsev[‡]

[†]L. V. Pisarzhevskii Institute of Physical Chemistry of the National Academy of Sciences of the Ukraine, Prospekt Nauki 31, Kiev 03028, Ukraine

[‡]N. S. Kurnakov Institute of General and Inorganic Chemistry, Russian Academy of Sciences, Leninsky Prospect 31, 119991 Moscow GSP-1, Russian Federation

[§]Equipe Organométalliques Matériaux et Catalyse, Institut des Sciences Chimiques de Rennes, UMR UR1-CNRS 6226, Université de Rennes 1, Campus de Beaulieu, 35042 Rennes Cedex, France

Supporting Information

ABSTRACT: Linking of the trinuclear pivalate fragment $Fe_2CoO(Piv)_6$ by the redox-active bridge $Ni(L)_2$ (compound **1**; LH is Schiff base from hydrazide of 4-pyridinecarboxylic acid and 2-pyridinecarbaldehyde, Piv^- = pivalate) led to formation of a new porous coordination polymer (PCP) $\{Fe_2CoO(Piv)_6\}\{Ni(L)_2\}_{1.5}$ (**2**). X-ray structures of **1** and **2** were determined. A crystal lattice of compound **2** is built from stacked 2D layers; the $Ni(L)_2$ units can be considered as bridges, which bind two $Fe_2CoO(Piv)_6$ units. In desolvated form, **2** possesses a porous crystal lattice (S_{BET} = 50 $m^2\ g^{-1}$, V_{DR} = 0.017 $cm^3\ g^{-1}$ estimated from N_2 sorption at 78 K). At 298 K, **2** absorbed a significant quantity of methanol (up to 0.3 $cm^3\ g^{-1}$) and chloroform. Temperature dependence of molar magnetic susceptibility of **2** could be fitted as superposition of $\chi_M T$ of $Fe_2CoO(Piv)_6$ and $Ni(L)_2$ units, possible interactions between them were taken into account using molecular field model. In turn, magnetic properties of the $Fe_2CoO(Piv)_6$ unit were fitted using two models, one of which directly took into account a spin−orbit coupling of Co^{II}, and in the second model the spin−orbit coupling of Co^{II} was approximated as zero-field splitting. Electrochemical and electrocatalytic properties of **2** were studied by cyclic voltammetry in suspension and compared with electrochemical and electrocatalytic properties of a soluble analogue **1**. A catalytic effect was determined by analysis of the catalytic current dependency on concentrations of the substrate. Compound **1** possessed electrocatalytic activity in organic halide dehalogenation, and such activity was preserved for the $Ni(L)_2$ units, incorporated into the framework of **2**. In addition, a new property occurred in the case of **2**: the catalytic activity of PCP depended on its sorption capacity with respect to the substrate. In contrast to homogeneous catalysts, usage of solid PCPs may allow selectivity due to porous structure and simplify separation of product.

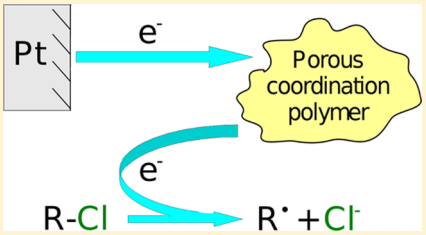

INTRODUCTION

Porous coordination polymers (PCPs) are promising candidates for creation of functional materials,[1] in particular, magnetic[2] and luminescent[3] materials, selective sorbents,[4] and catalysts for different types of reactions,[5] including electrochemical transformations of organic substrates.[6] The compounds of this class contain metal ions, which predetermine their magnetic or luminescent properties and catalytic activity, along with pores in the crystal lattice, which can give rise to selectivity due to molecules' discrimination by their size and shape.[7] Development of methods for assembling of PCPs with desired physical properties is an important task of modern inorganic and physical chemistry, as well as materials science. Synthesis and studies of new redox-active PCPs are attractive challenges due to the high potential of such a system in catalysis of redox reactions and creation of materials with tunable properties.[8] In particular, the redox-active PCPs, based on 3d metals, can be used instead of expensive Pd- or Ru-containing catalysts, for example, in dehalogenation of organic compounds.[9]

It can be expected that redox-active PCPs can be active in the processes of electrochemical dehalogenation of organic molecules similarly to synthesis of fluoro-containing compounds via freon conversion[10] as well as for preparation of various organic compounds[11] catalyzed by discrete soluble 3d

Received: December 29, 2013
Published: April 29, 2014

   dx.doi.org/10.1021/ic403167m | *Inorg. Chem.* 2014, 53, 4970−4979

metal complexes. In contrast to homogeneous catalysis, usage of the solid PCPs may allow researchers to simplify separation of the product and the catalyst, to achieve selectivity due to porous structure as well as to increase stability of the catalyst due to low probability of reactions between the activated catalytic species in the solution.[12]

Several methods for PCP creation on the basis of polynuclear "building blocks" were reported.[13] Previously we developed an approach to synthesis of PCP based on linking of pseudotrigonal trinuclear heterometallic pivalates by bi- or tripyridine bridges, which to a certain extent allowed us to predetermine composition and topology of the resulting compounds.[14] As an extension of these studies, we used a metal-containing redox-active bridge, previously reported[15] nickel(II) complex with Schiff base from hydrazide of 4-pyridinecarboxylic acid and 2-pyridinecarbaldehyde $Ni(L)_2$ (compound **1**). Besides having redox activity (*vide infra*) and availability of "free" donor atoms, capable of coordinating to other metal ions, $Ni(L)_2$ is stable in solutions[15] and possesses rigid geometry, which favors formation of PCP.

The aim of the present work was to study the catalytic activity of the redox-active PCP in the reactions of electrochemical dehalogenation of organic halides and to reveal the influence of substrate absorption by PCP on the catalytic performance of the system. In addition, in order to elucidate the influence of paramagnetic redox-active linker on magnetic properties of PCP, assembled from paramagnetic building blocks, as well as on redox properties (redox activity, redox potential, and reversibility of redox process) of such PCP, magnetic properties of the compounds were studied, and a thorough investigation of redox behavior of **1** and the coordination polymer, containing **1** as bridge, was carried out.

The choice of $Fe_2CoO(Piv)_6$ as the second component was motivated by its ability to form PCPs in combination with pyridine-containing bridges[14a] and electrochemical inertness, which was proven by us in a separate experiment.

In this Article, we report synthesis of new PCP $\{Fe_2CoO(Piv)_6\}\{Ni(L)_2\}_{1.5}$ (compound **2**), X-ray structures of **1** and **2**, and their physical and chemical properties. N_2 and methanol sorption isotherms were measured for desolvated **2**, and sorption of chloroform and 1,1,2-trifluoro-1,2,2-trichloroethane (freon R113) was estimated at pressures of saturated vapors of these halides (for $2{\cdot}9H_2O$, these results reflect water exchange by halide). Magnetic properties of **2** were studied, and numerical parameters of exchange interactions were calculated taking into account the spin−orbit coupling effects of Co^{II}. Electrochemical properties of **1** (in solution) and insoluble **2** (in suspension) were studied by cyclic voltammetry, and activity of these compounds in organic halides activation (dehalogenation) was shown.

EXPERIMENTAL SECTION

Materials. Reagents and solvents were commercially available (Aldrich, Merck, Labscan), in particular, anhydrous MeCN and DMF (Anhydroscan, 10 ppm of water), and were used without further purification, except compounds listed below. $CHCl_3$ was washed with K_2CO_3 water solution, distilled over P_2O_5, and stored over Linde type 4 Å molecular sieves in dark place. Freon R113, 1-iodobutane, and dibromomethane were distilled and stored in a dark place in a refrigerator. Et_4NBF_4 was purified by recrystallization and dried over P_2O_5. Compound $Fe_2CoO(Piv)_6(HPiv)_3$ was synthesized according to a previously reported procedure.[14d] Ligand LH (Schiff base from hydrazide of 4-pyridinecarboxylic acid and 2-pyridinecarbaldehyde) and compound **1** ($Ni(L)_2$) were synthesized as described.[15]

Synthesis of 2. A 0.026 g (0.05 mmol) portion of **1** and 0.037 g (0.033 mmol) of $Fe_2CoO(Piv)_6(HPiv)_3$ were dissolved in 2 mL of DMF in a test tube at 80−100 °C. The solution was cooled to room temperature, then 2 mL of DMF was accurately layered over the solution of reagents, and 40 mL of MeCN was layered over DMF. After a few days black crystals of $2{\cdot}Solv$ formed, which were collected by filtration, washed with MeCN, and dried in air. For analysis the sample was grounded in agate mortar. Anal. Calcd for $2{\cdot}9H_2O$, $CoFe_2Ni_{1.5}C_{66}H_{99}N_{12}O_{25}$: C, 46.1, H, 5.81, N, 9.78. Found C, 45.9, H, 5.34, N, 9.97. Yield 50% (0.028 g). Composition $2{\cdot}9H_2O$ corresponds to the compound in the form, stable in air.

X-ray Structure Determination. A single crystal of **1** was mounted on a Nonius four circle diffractometer equipped with a CCD camera and a graphite monochromated Mo Kα radiation source (Mo Kα radiation source, λ = 0.710 73 Å), from the Centre de Diffractométrie (CDFIX), Université de Rennes 1, France. A single crystal of **2** was mounted on a APEX II Bruker-AXS diffractometer for data collection (Mo Kα radiation source, λ = 0.710 73 Å), from the Centre de Diffractométrie (CDIFX), Université de Rennes 1, France. Structures of **1** and **2** were solved with a direct method using the SIR-97 program[16] and refined with a full matrix least-squares method on F^2 using the SHELXL-97 program.[17] Experimental details for physical characterization and complete crystal structure results as a CIF file including bond lengths, angles, and atomic coordinates are deposited as Supporting Information. CCDC 974475 and 974476 contain the supplementary crystallographic data for the compounds **1** and $2{\cdot}Solv$, respectively. These data can be obtained free of charge from the Cambridge Crystallographic Data Centre via www.ccdc.cam.ac.uk/data_request/cif). Single crystal data and structure refinement details for complexes **1** and **2** are presented in Table 1.

Table 1. Single Crystal Data and Structure Refinement Details for 1 and 2

	1	2
formula	$C_{24}H_{18}N_8NiO_2$	$C_{132}H_{162}Co_2Fe_4N_{24}Ni_3O_{32}$
M, g mol^{-1}	509.17	3114.25
cryst syst	monoclinic	orthorhombic
space group	$P2_1/a$	$Aba2$
a, Å	8.2395(2)	35.593(3)
b, Å	20.3085(9)	23.278(2)
c, Å	13.6924(5)	28.870(2)
β, deg	102.441(2)	90
V, Å^3	2237.37(14)	23 920(3)
Z	4	4
T, K	293(2)	150(2)
range of data collection	1.52−27.48	1.14−25.69
ρ_{calc}, g cm^{-3}	1.512	0.865
abs coeff, mm^{-1}	0.908	0.649
$F(000)$	1048	6480
collected reflns	9018	111 489
reflns unique	5121	20 879
R_{int}	0.0343	0.0672
GOF on F^2	1.069	1.090
R1[a] [$I > 2\sigma(I)$]	0.0443	0.0991
wR2[b] [$I > 2\sigma(I)$]	0.1048	0.2793
Flack param		0.21(2)

[a] $R1 = \Sigma||F_o| - |F_c||/\Sigma|F_o|$. [b] $wR2 = \{\Sigma[w(F_o^2 - F_c^2)^2]/\Sigma[w(F_o^2)^2]\}^{1/2}$.

Disordered solvent molecules could not be localized in X-ray structure of **2**, and corresponding electronic density was corrected by SQUEEZE procedure.[18] The solvent-accessible voids, the volume of which was estimated from the crystal lattice of **2**, could accommodate up to 10 molecules of DMF or 45 molecules of water per formula unit of **2**.

Methods. Thermogravimetric analyses (TGA) were performed in air on Q1500 instrument. Powder X-ray diffraction experiments were

dx.doi.org/10.1021/ic403167m | Inorg. Chem. 2014, 53, 4970−4979

performed on Bruker D8 instrument with Cu Kα radiation (λ = 1.540 56 Å). Nitrogen sorption measurements were performed by Sorptomatic-1990 instrument at 78 K. Absorption of methanol was measured gravimetrically, using a quartz microbalance (293 K). Each point on the absorption and desorption isotherms corresponds to equilibrium conditions (no change of sample weight at certain $P{\cdot}P_S^{-1}$). Prior to the measurements (both N_2 and methanol), in order to remove possible traces of DMF and other compounds,[19] which could be captured in the voids, a sample of **2**·9H_2O (composition of air-dry samples) was dried in vacuum, held in CH_2Cl_2 during 1 week; CH_2Cl_2 was changed several times into pure portions. Then the sample was dried in 10^{-3} Torr vacuum at 423 K (130 °C).

For assessment of $CHCl_3$, R113, or MeCN sorption by **2**, a portion of **2**·9H_2O in an open glass vessel was weighed and immersed into hermetically closed flask with excess of liquid organic substrate and allowed to stay overnight; then the flask was opened, and the glass vessel with **2** was quickly extracted, hermetically closed with lid of known weight, carefully wiped to clean all traces of liquid substrate from the external side, and weighed again. The same portion of **2**·9H_2O was used in all experiments; it was allowed to stay open overnight between the measurements. No special activation of the sample was performed.

Magnetic measurements were performed using a Quantum Design MPMS-XL SQUID magnetometer operating in the temperature range 2−300 K with a dc magnetic field up to 5 T. Powdered samples were measured in Teflon tape, and intrinsic diamagnetic corrections were calculated using Pascal's constants.[20]

In cyclic voltammetry (CV) experiments a glassy carbon (GC) disk (for DMF solutions) and a rough Pt plate (for suspension in MeCN) were used as working electrodes. Pt plate (with surface significantly higher than of the working electrode) was used as a counter electrode. ANE1 electrode (Ag wire in 0.1 M solution of $AgNO_3$ in MeCN)[21] was used as reference electrode. Potential of the ANE1 electrode was equal to −0.03 ± 0.02 V versus Fc^+/Fc couple (Fc = ferrocene, potential of Fc^+/Fc couple is +0.630 V vs normal hydrogen electrode[21]). CV experiments were carried out in Ar atmosphere. However, traces of oxygen could be present in some experiments, because excessive saturation with Ar was not desirable due to high volatility of organic halides (especially R113). Et_4NBF_4 was used as a background electrolyte. Before experiments the suspension of **2** was mixed using a magnetic stirrer, which was stopped immediately before CV scan. Unless explicitly specified, 0.100 V s^{-1} sweep rate was used. Data obtained in CV experiments of suspension (j vs E plots) were smoothed using adjacent averaging algorithm (10 points).

Unless explicitly declared, experiments with **1** performed in DMF solutions (c(**1**) = 5 mM) were provided on GC electrode, and experiments with **2** were performed in MeCN suspensions on Pt plate (m(**2**) = 0.010 g, V = 5 mL).

In order to compare results on different working electrodes, current density values j were used. The effective square of the polished GC electrode was supposed to be equal to geometrical one (3.14 mm^2), and effective square of the Pt plate was estimated from the geometrical square of GC electrode and proportion of the values of Fc anode currents on each electrode in the same Fc solution (found to be 37.81 mm^2).

Electrocatalytic experiments were provided in series. The substrate (R113, $CHCl_3$, n-C_4H_9I, or CH_2Br_2) was added stepwise to appropriate initial system in order to study current versus concentration dependencies. Total concentration of the substrate was calculated from the sum of all added portions during the series. Possible depletion of the substrate during consequent CV scans was neglected. The working electrode was polished with filter paper between the scans.

For product determination, preparative electrolysis of $CHCl_3$ in the presence of **2** was carried out using Pt plate as the working electrode, Mg plate as the counter electrode (sacrificial anode), and ANE1 as the reference electrode. A 300 μL portion of $CHCl_3$, 100 mg of **2**, and 35 mL of 0.1 M Et_4NBF_4 solution in MeCN were put in the hermetically closed cell, flushed with Ar for 15 min and processed for 6 h at potential 100 mV lower than E_c(**2**) upon continuous stirring. Mass spectra of the reaction mixture vapor or completely distilled reaction mixture were measured using SELMI MX-7304 A monopole mass-spectrometer (electron impact ionization).

RESULTS AND DISCUSSION

Synthesis. The strategy used for creation of the redox-active PCP was based on utilization of the redox-active mononuclear complex Ni(L)$_2$ (compound **1**, Figure 1 and Figures S1 and S2,

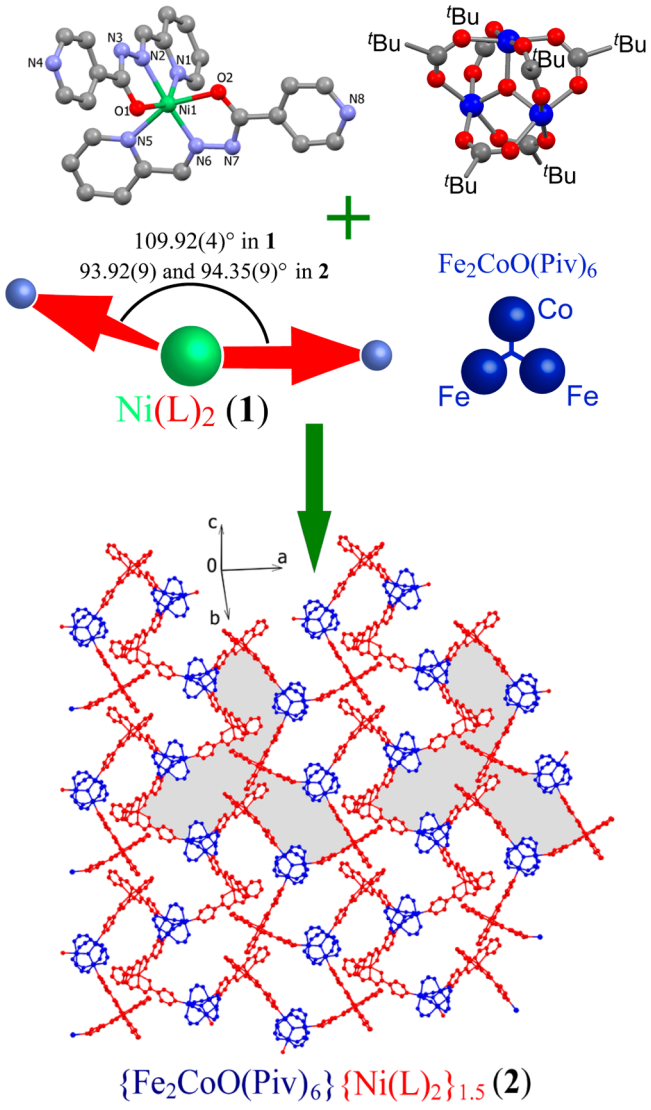

Figure 1. Formation of **2**·Solv by linking of **1** with $Fe_2CoO(Piv)_6$. Drawings of **1** and **2**·Solv represent their X-ray structures. One 2D layer is shown for **2**·Solv.

Supporting Information) as a linker between the trigonal trinuclear fragment $Fe_2CoO(Piv)_6$, where Piv^- is pivalate. Reaction of Ni(L)$_2$ with $Fe_2CoO(Piv)_6(HPiv)_3$ afforded the PCP {$Fe_2CoO(Piv)_6$}{Ni(L)$_2$}$_{1.5}$·9H_2O, hereafter referred to as compound **2**·9H_2O (composition of air-dry sample, see Experimental Section). Composition of **2** corresponds to one, expected from the ratio of potential coordination sites in $Fe_2CoO(Piv)_6$ (three potential vacations in the coordination spheres of three metal ions) and **1** (two N donors, able to coordinate to metal ion).

X-ray Structures. Molecular and crystal structures of both **1** and **2**·Solv were determined by single crystal X-ray diffraction

dx.doi.org/10.1021/ic403167m | Inorg. Chem. 2014, 53, 4970−4979

(exact solvent content in the single crystal could not be determined, see Experimental Section).

In **1** two anionic ligands L^- are coordinated to Ni^{II} cation, forming a neutral core (Figure 1). Ni^{II} ion is located in NiN_4O_2 chromophore, where two N atoms in *cis*-positions belong to pyridine groups, two N atoms in *trans*-positions are from azomethine groups, and two O atoms in *cis*-positions are from hydrazide groups.

Compound **2**·Solv possesses a structure of 2D polymer, in which the trinuclear $Fe_2CoO(Piv)_6$ building blocks are linked by **1** due to coordination of its 4-pyridine groups to Fe^{III} and Co^{II} ions (Figure 1 and Supporting Information Figures S3–S5). Three units of **1** are linked to each $Fe_2CoO(Piv)_6$ fragment, and in turn, each unit of **1** links the two trinuclear $Fe_2CoO(Piv)_6$ moieties. Both building blocks in **2**·Solv are not charged, so the polymeric framework is also neutral. The structure of $Ni(L)_2$ unit within the framework of **2**·Solv is similar to the structure of this block in individual compound **1** (Figure 1, more details of the X-ray structure discussion are presented in the Supporting Information).

The metal ions in $Fe_2CoO(Piv)_6$ are located in the vertexes of an almost equilateral triangle with M···M separations equal to 3.284(2), 3.285(2), and 3.322(2) Å. N–Ni–N angles (where N are nitrogen atoms of the pyridine groups, bound to the metal ions in $Fe_2CoO(Piv)_6$) in $Ni(L)_2$ units within the framework of **2** are equal to 93.92(9)° and 94.35(9)°. These values are less than the respective angle in **1** (109.92(4)°), so linking of $Ni(L)_2$ by the trinuclear carboxylate led to some distortion of this mononuclear building block compared to its geometry in the nonbonded state. This angle change was associated with nonsystematic and insignificant changes of the other angles in NiN_4O_2 chromophores in $Ni(L)_2$ within **2** compared to respective values in **1** (Tables S1 and S2, Supporting Information).

In contrast with previously reported cases, where linking of trigonal $Fe_2MO(Piv)_6$ (M^{II} = Co, Ni) units by linear 4,4-bipyridine (bipy) or *trans*-bis(4-pyridine)-1,2-ethylene (dpe) bridges led to formation of planar 2D honeycombs $Fe_2MO(Piv)_6(bipy)_{1.5}$ or $Fe_2MO(Piv)_6(dpe)_{1.5}$,[14b–d] a combination of the same trigonal particles with "angular" bridges $Ni(L)_2$ caused formation of nonplanar 2D layers (Supporting Information Figure S3). This is consistent with geometry of the $Ni(L)_2$ linker: the angle between "binding directions" of 4-pyridine groups in **1** is close to 90° (Figure 1 and Supporting Information Figure S5), which makes impossible the formation of planar $[\{Fe_2MO(Piv)_6\}\{bridge\}]_n$ rings. Notably, both in zigzag 2D layers of **2** and in honeycomb 2D layers of $Fe_2MO(Piv)_6(bipy)_{1,5}$ or $Fe_2MO(Piv)_6(dpe)_{1,5}$, cyclic fragments consisting of six links $\{Fe_2MO(Piv)_6\}\{bridge\}$ can be distinguished (Figure 1, mentioned cycle is highlighted by gray color).

Crystal lattice of **2** is formed by parallel 2D undulating layers (Figure 1) which alternate along the *b* axis (two layers being symmetrical thanks to a glide plane *a* parallel to (400)), thus forming the porous lattice (Figure 2 and Supporting Information Figures S6 and S7). These pores are filled by disordered solvent.

Thermal Behavior and Sorption Properties of 2. On heating to 280 °C compound **2**·$9H_2O$ gradually lost up to 10% of weight, which corresponded to elimination of nine water molecules (theoretical weight loss is 9.4%). Further temperature growth led to decomposition of the compound (Supporting Information Figure S8). Weight loss stabilized at

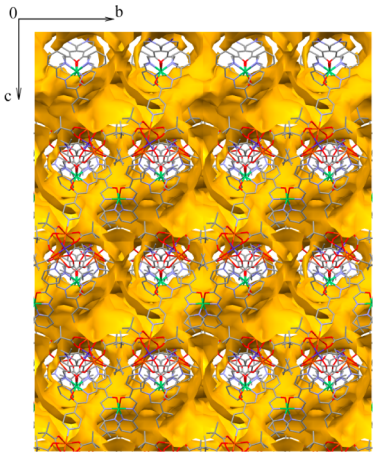

Figure 2. Visualization of voids in **2** by Mercury software[22] for a probe molecule with r = 1.4 Å (projection along *a* axis).

570 °C and was equal to 81% (corresponding to formation of $CoFe_2O_4$ and NiO, theoretical weigh loss is 80%). Crystals of **2**·Solv, taken from the matrix solution, upon exposure to air and grinding, undergo desolvation, resulting in disorder of the crystal structure, as evidenced by powder X-ray diffraction of **2**·$9H_2O$ (Supporting Information Figure S9).

Desolvation of **2**·Solv resulted in a decrease of pore volume (V_{DR} = 0.017 $cm^3\ g^{-1}$ and S_{BET} = 50 $m^2\ g^{-1}$ as determined from N_2 adsorption isotherm at 78 K, see Supporting Information Figure S10, compared to 0.54 $cm^3\ g^{-1}$, estimated by Platon software[23] for a probe molecule with r = 1.4 Å for single crystal). In contrast, a desolvated sample of **2** absorbed about 0.3 $cm^3\ g^{-1}$ of methanol from the gas phase at $P{\cdot}P_S^{-1}$ = 0.94 and T = 298 K (Supporting Information Figure S10), which was about 55% of volume, occupied by solvent in as-synthesized single crystals. High methanol sorption capacity compared to N_2 at 78 K along with wide hysteresis of methanol absorption–desorption and can provide evidence for flexibility of the crystal lattice of this PCP. Interaction of the lattice of **2** with methanol probably leads to its partial expansion, similar to reported cases.[24]

Compound **2** absorbed approximately 20 molecules (0.93 $cm^3\ g^{-1}$) of $CHCl_3$, approximately 2 molecules (0.14 $cm^3\ g^{-1}$) of R113, or approximately 10 molecules (0.34 $cm^3\ g^{-1}$) of MeCN per formula unit from gas phase (air + substrate vapor, see Experimental Section).

Magnetic Properties of 2·$9H_2O$. Magnetic properties of **2**·$9H_2O$ were characterized by magnetic molar susceptibility, χ_M, measurements in 2–300 K temperature range (Figure 3), and were typical for antiferromagnetically coupled trinuclear carboxylates,[14b–d,25] except that $\chi_M T$ values were increased due to the contribution of paramagnetic ion (Ni^{II}), not involved in the exchange interactions. Simulation of $\chi_M T$ versus T dependency for **2**·$9H_2O$ was performed using an additive model, where $\chi_M T$ of **2**·$9H_2O$ was considered as a superposition of magnetism attributed to both blocks, resulting in a sum of $\chi_M T$ values of trinuclear and mononuclear fragments with corresponding coefficients (1 and 1.5, respectively) according to the composition of **2** (eq 1).

$$\chi_M T = \chi_M T(Fe_2Co) + 1.5\chi_M T(Ni) \quad (1)$$

Possible intermolecular interactions between $Fe_2CoO(Piv)_6$ and $Ni(L)_2$ were taken into account using a molecular field model.[20]

dx.doi.org/10.1021/ic403167m | Inorg. Chem. 2014, 53, 4970–4979

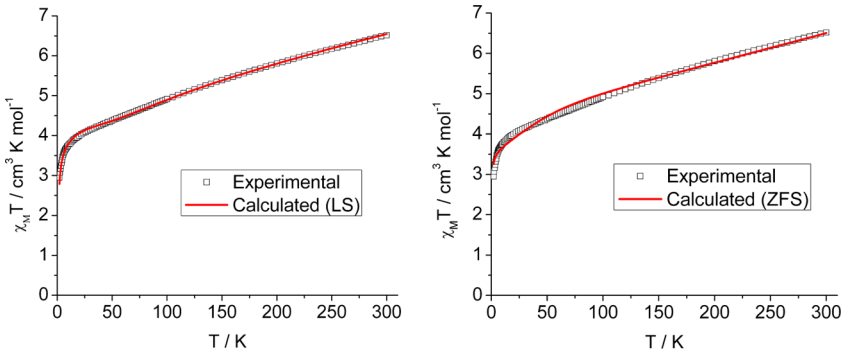

Figure 3. $\chi_M T$ vs T dependency for **2**·9H$_2$O (points) and the calculated curve within a model based on the Hamiltonian in eq 2 (a) and the Hamiltonian in eq 4(b). Parameters, which correspond to these curves, are presented in the text.

$\chi_M T$(Fe$_2$Co) was calculated in the frames of spin-Hamiltonian (eq 2), that directly took into account Co^{II} level splitting due to spin−orbit coupling.

$$H = -2J_{FeFe}\hat{S}_{Fe1}\cdot\hat{S}_{Fe2} - 2J_{FeCo}(\hat{S}_{Fe1} + \hat{S}_{Fe2})\cdot\hat{S}_{Co} + g_{Fe}\beta(\hat{S}_{Fe1} + \hat{S}_{Fe2})\cdot H + \Delta\left[\hat{L}_z^2 - \frac{1}{3}L(L+1)\right] - \frac{3}{2}\kappa\lambda\hat{L}\hat{S} + \beta\left[\left(-\frac{3}{2}\kappa\hat{L}\right)H + g_{Co}\left(\hat{S}_{Coz} + \hat{S}_{Coxy}\right)H\right] \quad (2)$$

where $\hat{S}_{Fe1}$,$\hat{S}_{Fe2}$, $\hat{S}_{Co}$ are the spin operators for trinuclear exchange cluster, J_{FeFe} describes the exchange between two iron ions, and J_{FeCo} is that between each iron ion and the cobalt ion.

Calculations were performed by full-matrix diagonalization using Mjöllnir software,[26] previously reported[14c,27] by us and specially improved (version 0.3) in order to allow splitting the considered model into a few noninteracting blocks (trinuclear Fe$_2$Co block and mononuclear Ni(L)$_2$) and treating them separately.

$\chi_M T$(Ni) was considered temperature-independent and calculated using eq 3

$$\chi_M T(\mathrm{Ni}) = 0.1251\cdot g_{Ni}{}^2\cdot S(S+1) \quad (3)$$

where S = 1.

The best correspondence of experimental and calculated curves was obtained at the following parameters' values: J_{FeFe} = −70 cm^{-1}, J_{CoFe} = −22 cm^{-1}, Δ = 500 cm^{-1}, κ = 0.93, λ = −170 cm^{-1}, g_{Fe} = 2.0 (fixed to avoid overparametrization), g_{Co} = 2.2, g_{Ni} = 2.3, zJ' = −0.23 cm^{-1}, g(mol field) = 2.0, tip = 0.0018 (R^2 = 4.7 × 10^{-5}, where $R^2 = \sum[(\chi_M T)_{obs} - (\chi_M T)_{calcd}]^2/\sum(\chi_M T)_{obsd}{}^2$).

An alternative approach to take spin−orbit coupling of Co^{II} into account (more widely used due to its simplicity[28]) is based on zero-field splitting spin-Hamiltonian (eq 4), where spin−orbit coupling was considered by an effective zero-field splitting term.

$$H = -2J_{FeFe}\hat{S}_{Fe_1}\cdot\hat{S}_{Fe_2} - 2J_{FeCo}(\hat{S}_{Fe_1}\hat{S}_{Co} + \hat{S}_{Fe_2}\hat{S}_{Co}) + g_{Co_{xy}}\beta\hat{S}_{Co_{xy}}H + g_{Co_z}\beta\hat{S}_{Co_z}H + g_{Fe}\beta(\hat{S}_{Fe_1} + \hat{S}_{Fe_2})\cdot H + D\left(\hat{S}_{Co_z}^2 - \frac{1}{3}S_{Co}(S_{Co}+1)\right) \quad (4)$$

In the Hamiltonian in eq 4, the first line corresponds to the superexchange interactions between Heisenberg spins localized at the metal sites (J_{FeFe} and J_{FeCo}), the second line corresponds to the anisotropic or isotropic interactions between the local spins and the external field through Zeeman interactions (g_{Co} and g_{Fe}), respectively, and the third line corresponds to zero-field splitting of the spin levels of Co^{II}.

This method can be used in the case of high Δ, when only two levels with M_s = $^3/_2$ and M_s = $^1/_2$ are noticeably occupied.[27] The results of the $\chi_M T$ versus T fit based on this approach are the following: J_{FeFe} = −63.0 cm^{-1}, J_{CoFe} = −32.5 cm^{-1}, D = 70 cm^{-1}, g_{Fe} = 2.0 (fixed to avoid overparametrization), g_{Coz} = 2.0, g_{Coxy} = 3.12, g_{Ni} = 2.3, tip = 0.0022 (R^2 = 3.2 × 10^{-4}).

Both J_{FeFe} and J_{CoFe} in **2**·9H$_2$O are lower (in absolute values) than the respective values for other complexes, containing Fe$_2$CoO(Piv)$_6$ unit and pyridine-containing ligands 4,4′-bipyridine or *trans*-bis(4-pyridine)-1,2-ethylene,[14b−d] 2,2′-bipyridine, 2,2′-bipyrimidine[29] and 2,2′-azopyridine or 2,3-di(2-pyridyl)-quinoxaline.[30] This can be attributed to the presence of the electron-accepting C═O group in the fourth position of pyridine ring, coordinated to Fe^{III} or Co^{II} ions in **2**·9H$_2$O, which can contribute to decrease of J compared to its analogues due to relative decrease of electronic density on Fe$_2$CoO(Piv)$_6$ unit. A similar influence of electron-accepting groups in carboxylates on J values in trinuclear complexes of this type was also found.[25,27]

Electrochemical and Electrocatalytic Properties of 1 and 2. The cyclic voltammogram of **1** in DMF on the glassy carbon (GC) electrode revealed two consequent redox processes at $E_{1/2}$ = −1.81 and −2.14 V (all potentials are referred vs 0.1 M AgNO$_3$|Ag (ANE1) electrode, see Figure S11 and S12 in Supporting Information). These processes could be assigned to Ni(L)$_2$/Ni(L)$_2^-$ and Ni(L)$_2^-$/Ni(L)$_2^{2-}$ redox couples, respectively. The process at $E_{1/2}$ = −1.81 V was reversible and one-electron (ΔE = 60 mV; average value of $j_c\cdot j_a^{-1}$ for different scans was 1.0 ± 0.2 for scans to −2.0 V, the deviation of $j_c\cdot j_a^{-1}$ from unity for this process was higher when two consequent reductions were included in one scan). The

dx.doi.org/10.1021/ic403167m | Inorg. Chem. 2014, 53, 4970−4979

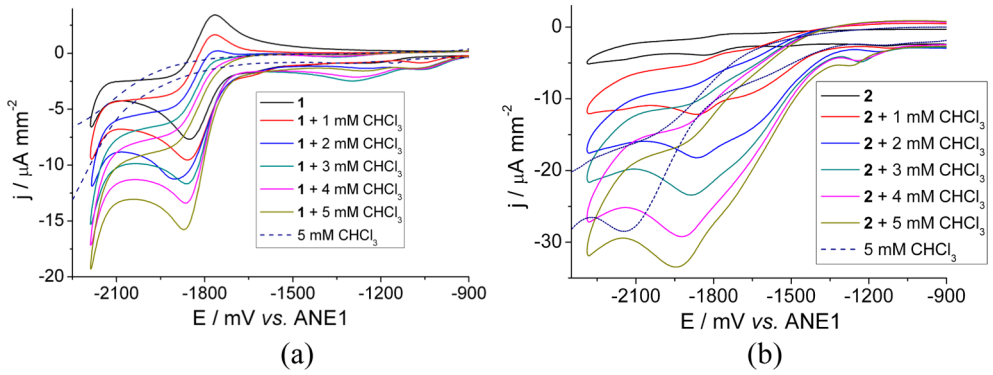

Figure 4. CV curves for the solutions of **1** in DMF, **1** in the solutions of $CHCl_3$ in DMF, along with the solution of $CHCl_3$ in DMF without **1** (a). The suspension of **2** in MeCN, the suspension of **2** in the solutions of $CHCl_3$, along with the solution of $CHCl_3$ in MeCN without **2** (b). In all experiments $c(\mathbf{1})$ = 5 mM (if present) or $m(\mathbf{2})$ = 0.010 g (if present) in 5 mL of the solution, the background electrolyte Et_4NBF_4, ν = 0.1 V s^{-1}.

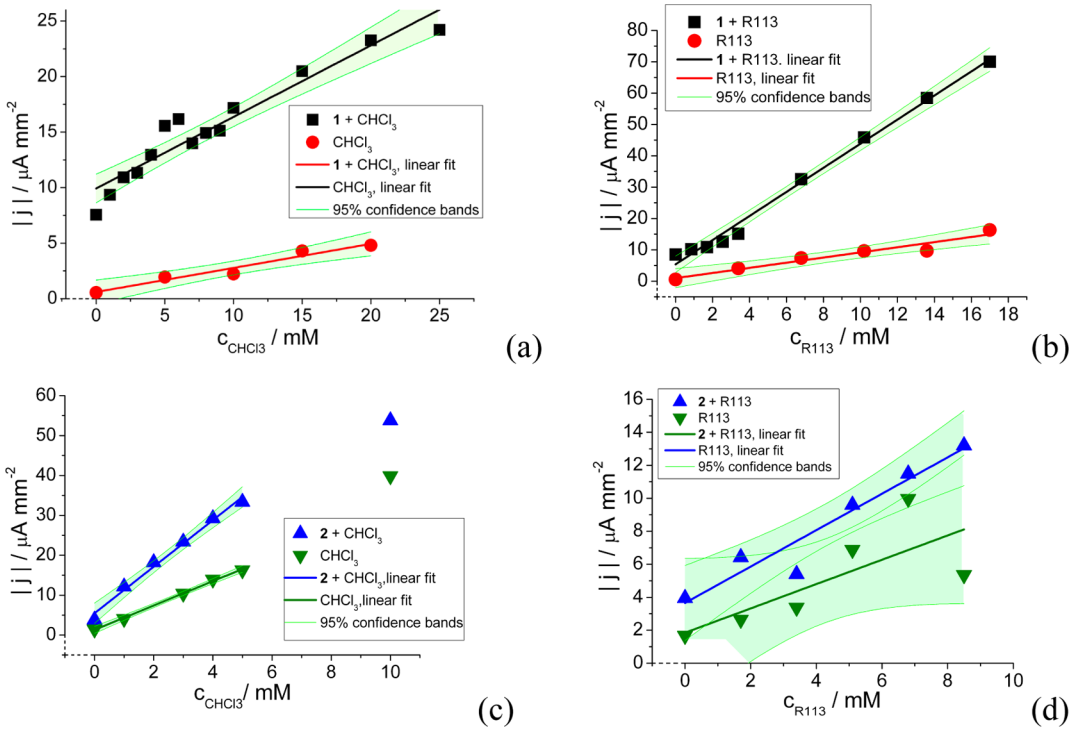

Figure 5. Plots of peak j values for **1** (a, b; GC electrode) or **2** (c, d; Pt electrode) vs the halide concentration and j values for $CHCl_3$ or R113 at appropriate potentials vs their concentration along with linear fits and 95% confidence bands.

single-electron nature of the process at $E_{1/2}$ = −1.81 V was also confirmed by estimation of diffusion coefficient, which adopted reasonable value $D = 2 \times 10^{-6}$ cm^2 s^{-1} only for n = 1 (calculated from current values[31] at different scan rates, Supporting Information Figure S11b). The value of D is consistent with the values, reported for other coordination compounds.[32] For the second process (at −2.14 V) $j_c \cdot j_a^{-1}$ exceeded 2.0, providing evidence for its poor reversibility.

The reduction of $Ni(L)_2$ is probably ligand-based, as it can be concluded from comparison with CV curve for the ligand (Supporting Information Figure S12) and similar systems.[33] Notably, the reduction process in solution of ligand (E_c = −2 V) was irreversible in the range of sweep rate up to 5.0 V s^{-1}, in contrast to such a process in **1**. The effect of organic halides electroactivation, $CHCl_3$, $CF_2ClCFCl_2$ (freon R113), n-C_4H_9I, and CH_2Br_2, was shown only for redox couple at $E_{1/2}$ = −1.81 V in **1**, while examination of LH as mediator of the organic substrate dehalogenation was not carried out because of irreversibility of its reduction.

Electrochemical properties of the solid compound **2** were studied using a rough Pt plate electrode immersed into a suspension of fine powder of **2** in MeCN. MeCN was chosen as a medium for experiments with **2**, because this PCP was stable in this solvent, but dissolved in DMF with apparent destruction of polymeric chains (however, solubility of **1** in MeCN was not sufficient for high-quality CV measurements; the results of CV of **1** in MeCN on Pt electrode are presented in the Supporting Information). Previously redox properties of solids were successfully studied in suspensions.[6e,34] Alternative reported methods involved preparation of paste electrodes,[35] and deposition of thin films on metal[6b,36] or carbon material (graphite or glassy carbon)[37] electrodes, but we could not detect redox processes of **2** in graphite paste, while the results of CV experiments (peak current values) with thin films of **2**

dx.doi.org/10.1021/ic403167m | Inorg. Chem. 2014, 53, 4970−4979

deposited on Pt electrode were not reproducible. Compound **2** showed distinct reduction peak at E_c = −1.82 V, with less pronounced oxidation at E_a = −1.72 V (Figure 4 and Supporting Information Figure S12), which could be assigned to reduction and oxidation of $Ni(L)_2$ bound in the polymeric lattice of **2**. Though the difference of redox potentials of **2** compared to **1** could be caused by electronic influence of coordinated $Fe_2CoO(Piv)_6$ unit or different solvent, different electron transfer kinetics seem to be a more significant reason that governs change of redox behavior (especially the values of cathodic and anodic currents). Magnetochemical studies also suggested that the interactions between $Fe_2CoO(Piv)_6$ and NiL_2 unit were not significant, since magnetic susceptibility versus T dependency for **2** could be fitted as superposition of contributions of these building blocks (*vide supra*).

It could be expected that the current values (presented as the current density, j) for the suspensions of **2** had to be lower than j values for the solutions of **1**, if only Ni^{II} ions from the surface layer are involved in the redox process. However, j values in the case of the suspension of **2**, which contained 1.75 mM of $Ni(L)_2$ incorporated in the coordination polymer, were comparable to j found in 5 mM solution of **1** (Figure 5). Noticeable adhesion of **2** suspension to the working electrode was observed, and it also cannot be excluded that $Ni(L)_2$ moieties in **2** undergo the redox transformation not only on the surface of particles, but the "internal" sites are involved.

Electrocatalytic dehalogenation of the organic halides was evaluated by growth of the current of cathodic peaks in CV of **1** and **2** in the presence of corresponding substrates ($CHCl_3$ and R113 for **1** and **2**, Figure 4, and in addition[38] *n*-C_4H_9I and CH_2Br_2 for **1**, Supporting Information Figure S13). Catalytic activity of coordination compounds in electrochemical reactions is based on electron transfer by the reduced form of the complex to organic substrate at a potential, which is less negative than the potential of such substrates, in particular freon,[39] reduction at absence of the mediator. Such activation of organic substrate results in growth of cathodic current of coordination compound due to electron consumption for regeneration of the reduced form of mediator. The organic substrate in such process is reduced by mediator and may not undergo direct reduction on electrode. Electrochemical reduction of R−Hal leads to generation of radical $R^{\bullet}$ and then anion R^- in one- or two-electron reactions, respectively, which is rate-limiting stage.[40] The further reaction pathway depends on its structure, as was studied in detail previously.[39,41] The most typical transformations of R^- are the following: (i) capture of proton, leading to formation of RH[42] (proton is usually eliminated from tetraalkylammonium cations, added as background electrolyte[43]), (ii) elimination of another halide anion, leading to formation of alkene[44] (clearly, only anions containing two or more carbon atoms can undergo such transformation), (iii) dimerization of radicals.[44] CH_2Cl_2 and Cl^- were found as the products of $CHCl_3$ dehalogenation in the presence of **2**; the details of the products determination are presented in Experimental Section and Supporting Information (Figures S14−S16).

Peak current density values j were used for assessment of electrocatalytic activity of **1** and **2**. These values were calculated from CV curves at E_c potentials separately for each curve. E_c values of **1** or **2** in the presence of organic halide slightly shifted toward negative potentials, and such a shift increased with growing concentration of the halide. Among studied organic halides, R113 and $CHCl_3$ undergo reduction at above-mentioned E_c potentials even without catalyst, so in order to take into account this noncatalytic reduction, for each halide concentration a control experiment with the same concentration of the halide in absence of **1** or **2** was performed. For each concentration of halide a control value of noncatalytic current density j in the absence of **1** or **2** was taken as j at E_c value of the appropriate curve at the same halide concentration in the presence of **1** or **2**.

Addition of $CHCl_3$ to a solution of **1** led to growth of peak j, which was linear up to $c(CHCl_3)$ = 26 mM (Figures 4 and 5). The slope of the j versus $c(CHCl_3)$ plot was 0.6 ± 0.2 $\mu A\ mm^{-2}\ mM^{-1}$. j growth, caused by reduction of $CHCl_3$ at the same potentials in absence of **1**, was significantly lower (slope is 0.22 ± 0.05 $\mu A\ mm^{-2}\ mM^{-1}$). A similar situation took place in the case of **1** and R113 (Figure 5; slopes of j versus c(R113) plots were 3.8 ± 0.3 and 0.8 ± 0.2 $\mu A\ mm^{-2}\ mM^{-1}$ in the presence and absence of **1**, respectively), as well as *n*-C_4H_9I and CH_2Br_2 (Supporting Information Figure S18). These findings provided definite statistically significant evidence, that **1** catalyzed dehalogenation of all these organic halides in solution.

In solutions, containing **1**, linear dependency of j on halide concentration was observed in the whole range of studied concentrations of R113, $CHCl_3$ and *n*-C_4H_9I, but an increase of CH_2Br_2 concentration above *ca.* 15 mM did not lead to significant j growth. Similar "saturation" of catalytic current at increasing substrate concentration was previously observed in the case of electrocatalytic oxidation of ethanol.[45] Also, the values of j were ca. 2 times higher in the case of R113 compared to $CHCl_3$ and CH_2Br_2, and ca. 10 times higher compared to the case of *n*-C_4H_9I (at similar halide concentrations, Figure 5 and Supporting Information Figure S18). This difference can be explained by different electron transfer efficiency in these systems, which seems to be higher in the case of R113 compared to $CHCl_3$, *n*-C_4H_9I, and CH_2Br_2, and is consistent with separation between redox potential of catalyst **1** and halide (see Supporting Information for details): increase of separation between redox potentials leads to less efficient electron transfer and lower values of catalytic current (Figure 6). Such behavior is typical for systems with outer sphere electron transfer mechanism, and this conclusion is consistent with the structure of **1** (coordinatively saturated Ni ion).

The opposite situation (compared to solutions of **1**) was observed in the case of the suspension of **2**. While for $CHCl_3$ the situation was similar to the case of solution of **1** (peak j values increased linearly with slopes 5.8 ± 0.6 and 3.1 ± 0.2 μA

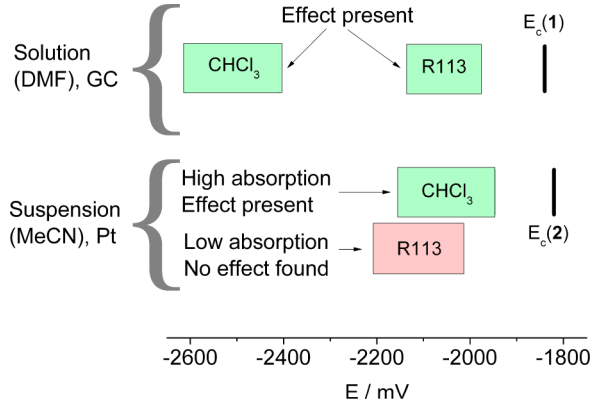

Figure 6. Catalytic activity of **1** and **2** vs redox potentials of the catalysts and the halides and vs the halides' sorption by **2**.

dx.doi.org/10.1021/ic403167m | *Inorg. Chem.* 2014, 53, 4970−4979

mm^{-2} mM^{-1} in the presence and absence of **2**, respectively), addition of R113 to **2** did not result in significantly different growth of *j* compared to *j* in control experiments with the solutions of R113 (Figures 4 and 5, and Supporting Information Figures S19 and S20). Thus, catalytic effect can be considered to be statistically significant for the case of $CHCl_3$ electroactivation by **2**; however, no reliable evidence for R113 activation was found in this case.

In a separate experiment, a suspension of **2** in MeCN was filtered, and the filtrate was studied by CV in order to confirm that this coordination polymer did not dissolve in MeCN. No peaks were found in CV of the filtrate, confirming that the redox process observed in the suspension of **2** was caused by solid particles of this polymer, but not by soluble compounds, which could appear due to their dissolving or degradation. Addition of $CHCl_3$ to the filtrate led to electrochemical behavior, close to the behavior of $CHCl_3$ solutions in absence of **2**.

Probably, the activation of $CHCl_3$ molecule involves the following steps: (i) absorption of the molecule by a particle of **2**; (ii) adhesion of the particle to working electrode; (iii) electron transfer from working electrode to the particle (with reduction of one or more NiL_2 blocks); (iv) electron transfer from the particle to the absorbed $CHCl_3$ molecule. Compound **2** showed good adhesion to Pt electrode (*vide supra*), which probably facilitated electron transfer.

Though many reasons can be responsible for different sorption capacity of **2** with respect to $CHCl_3$ and R113, there is clear correlation between electrocatalytic activity of **2** and its sorption capacity. At the same time, no conclusions about possible correlation between electrocatalytic activity of **2** and the difference between E_c of this PCP and reduction potential of halide can be made, because redox potentials of $CHCl_3$ and R113 on Pt electrode in MeCN are quite close (see Figure 6 and comments on redox behavior of halides in Supporting Information).

Electrocatalytic activity of complexes of 3d metals in the majority of reported cases was associated with substrate coordination to metal ion in an intermediate-reduced form of coordination compound.[10,46] The cases when coordination of substrate to electrocatalyst was not possible are quite scarce.[47] Taking into account probable ligand-centered nature of the catalytically active redox processes in **1** and **2** and high stability constant of $Ni(L)_2$,[15] it can be supposed that the electroactivation of $CHCl_3$ and R113 on reduced forms of **1** and **2** occurred due to ligand-to-substrate electron transfer without coordination of the substrate to Ni^{II}. This supposition is supported by the correlation between catalytic current values and the difference between redox potential of **1** and halide (*vide supra*).

To the best of our knowledge, compound **2** is the first reported solid-phase electrocatalyst of organic compound dehalogenation. The efficiency of solid coordination polymers as the catalysts of different electrochemical reactions can be compared on the basis of relative current growth upon addition of substrate, which can provide evidence for the efficiency of electron transfer to substrate. In the case of **2** total current increased from 145 to 1265 μA upon addition of 5 mM of $CHCl_3$; however, only 555 μA increase can be undoubtedly attributed to catalytic current (it cannot be definitely excluded that 560 μA growth was caused by direct reduction of $CHCl_3$ on electrode surface). So, we can conclude that current growth is at least 3-fold, which is comparable with relative increase of current in the processes of electrocatalytic ethanol oxidation, methanol carbonylation to dimethylcarbonate, and CO_2 reduction to oxalic acid, catalyzed by solid MOFs.[6d−f] In contrast, a significantly higher increase of current (7-fold and more) was found in reactions of oxidation of H_2O_2 or oxygen reduction on solid MOFs.[6g,h]

CONCLUSIONS

In the result of this study it was shown that the redox-active complex **1** preserved its activity being incorporated in the coordination polymer **2** as building block with insignificant change of redox potential. The method for redox-active PCP creation was developed. This finding opens the way to directed synthesis of PCPs, possessing desired redox properties. The use of bridging unit $Ni(L)_2$ with close to 90° angle between "linking directions" in combination of trigonal trinuclear pivalate $Fe_2CoO(Piv)_6$ resulted in formation of nonplanar 2D layers, the structure of which was significantly distorted compared to planar regular honeycomb, previously found in the case of linear or trigonal bridges. It was shown that magnetic properties of **2** were mainly determined by magnetism of the trinuclear pivalate and the $Ni(L)_2$ bridge, while interactions between these components were minor. Redox activity of solid **2** was successfully studied in suspension in MeCN, and it was proven that the observed redox processes could not be caused by soluble species, but originated from solid particles. Redox potential of $Ni(L)_2$ incorporated in **2** was close to the value of the redox potential of this compound in solution, providing evidence that electronic influence of $Fe_2CoO(Piv)_6$ on $Ni(L)_2$ was not significant; this observation is consistent with the result of magnetochemical studies. Both **1** in solution and **2** in suspension showed catalytic activity in $CHCl_3$ dehalogenation, and **1** also was catalytically active in dehalogenation of R113, n-C_4H_9I, and CH_2Br_2 in solution. Electrocatalytic activity of **1** and **2** probably involved electron transfer without substrate coordination to the metal ion. The results of this study are important for creation of new redox-active PCPs, development of heterogeneous electrocatalysts, as well as catalysis of redox reactions.

ASSOCIATED CONTENT

Supporting Information

X-ray crystallographic files, in CIF format (CCDC 974475 (**1**) and 974476 (**2**)); additional details of X-ray structures description; tables presenting lengths of selected bonds in **1** and in $Ni(L)_2$ unit in **2**, values of some angles in **1** and in $Ni(L)_2$ unit in **2**; text with comments on redox behavior of $CHCl_3$, R113, n-C_4H_9I, CH_2Br_2, and **1**; comments on determination of products of $CHCl_3$ dehalogenation at presence of **2**; figures with formula of LH; additional figures for X-ray structures description; TG curve for $\mathbf{2}\cdot 9H_2O$; powder XRD data; graphs of N_2 and methanol adsorption by **2**; mass spectra of the reaction mixture after preparative electrolysis; and additional figures demonstrating experimental CV data and current vs halide concentration plots for n-C_4H_9I and CH_2Br_2. This material is available free of charge via the Internet at http://pubs.acs.org.

AUTHOR INFORMATION

Corresponding Authors

*E-mail: svk001@mail.ru. Phone: +38(044)5256661. Fax: +38(044)5256216.

*E-mail: ilerem@igic.ras.ru. Phone: +7(495)9522084. Fax: +7(495)9541279.

Notes

The authors declare no competing financial interest.

■ ACKNOWLEDGMENTS

This work was supported by a joint grant of the National Academy of Sciences of Ukraine and Russian Foundation for Basic Research (No. 10-03-12U and 10-03-13U), Russian Foundation for Basic Research (No. 14-03-90423), Russian Academy of Sciences, and the National Academy of Sciences of Ukraine, the Council on Grants of the President of the Russian Federation (Grant NSh-4773.2014.3), CNRS, University of Rennes 1, Région Bretagne, and FEDER. The authors thank Dr. R. A. Polunin and P. S. Yaremov for their assistance with sorption measurements and I. B. Bychko for assistance with mass-spectral measurements.

■ REFERENCES

(1) (a) Wang, C.; Liu, D.; Lin, W. *J. Am. Chem. Soc.* **2013**, *135*, 13222−13234. (b) Champness, N. R. *Dalton Trans.* **2011**, *40*, 10311−10315. (c) Kuppler, R. J.; Timmons, D. J.; Fang, Q.-R.; Li, J.-R.; Makal, T. A.; Young, M. D.; Yuan, D.; Zhao, D.; Zhuang, W.; Zhou, H.-C. *Coord. Chem. Rev.* **2009**, *253*, 3042−3066.

(2) (a) Kurmoo, M. *Chem. Soc. Rev.* **2009**, *38*, 1353−1379. (b) Dechambenoit, P.; Long, J. R. *Chem. Soc. Rev.* **2011**, *40*, 3249−3265. (c) Coronado, E.; Espallargas, G. M. *Chem. Soc. Rev.* **2013**, *42*, 1525−1539. (d) Kolotilov, S.; Kiskin, M.; Eremenko, I.; Novotortsev, V. *Curr. Inorg. Chem.* **2013**, *3*, 144−160.

(3) Allendorf, M. D.; Bauer, C. A.; Bhakta, R. K.; Houk, R. J. T. *Chem. Soc. Rev.* **2009**, *38*, 1330−1352.

(4) Zou, R.; Abdel-Fattah, A. I.; Xu, H.; Zhao, Y.; Hickmott, D. D. *CrystEngComm* **2010**, *12*, 1337−1353.

(5) (a) Ma, L.; Abney, C.; Lin, W. *Chem. Soc. Rev.* **2009**, *38*, 1248−1256. (b) Lee, J.; Farha, O. K.; Roberts, J.; Scheidt, K. A.; Nguyen, S. T.; Hupp, J. T. *Chem. Soc. Rev.* **2009**, *38*, 1450−1459. (c) Janiak, C.; Vieth, J. K. *New J. Chem.* **2010**, *34*, 2366−2388. (d) Farrusseng, D.; Aguado, S.; Pinel, C. *Angew. Chem., Int. Ed.* **2009**, *48*, 7502−7513.

(6) (a) Thorum, M. S.; Yadav, J.; Gewirth, A. A. *Angew. Chem.* **2009**, *121*, 171−173. (b) Babu, K. F.; Kulandainathan, M. A.; Katsounaros, I.; Rassaei, L.; Burrows, A. D.; Raithby, P. R.; Marken, F. *Electrochem. Commun.* **2010**, *12*, 632−635. (c) Pintado, S.; Goberna-Ferrón, S.; Escudero-Adán, E. C.; Galán-Mascarós, J. R. *J. Am. Chem. Soc.* **2013**, *135*, 13270−13273. (d) Yang, L.; Kinoshita, S.; Yamada, T.; Kanda, S.; Kitagawa, H.; Tokunaga, M.; Ishimoto, T.; Ogura, T.; Nagumo, R.; Miyamoto, A.; Koyama, M. *Angew. Chem., Int. Ed.* **2010**, *49*, 5348−5351. (e) Jia, G.; Gao, Y.; Zhang, W.; Wang, H.; Cao, Z.; Li, C.; Liu, J. *Electrochem. Commun.* **2013**, *34*, 211−214. (f) Kumar, R. S.; Kumar, S. S.; Kulandainathan, M. A. *Electrochem. Commun.* **2012**, *25*, 70−73. (g) Zhang, C.; Wang, M.; Liu, L.; Yang, X.; Xu, X. *Electrochem. Commun.* **2013**, *33*, 131−134. (h) Mao, J.; Yang, L.; Yu, P.; Wei, X.; Mao, L. *Electrochem. Commun.* **2012**, *19*, 29−31.

(7) (a) Czaja, A. U.; Trukhan, N.; Müller, U. *Chem. Soc. Rev.* **2009**, *38*, 1284−1293. (b) Bux, H.; Liang, F.; Li, Y.; Cravillon, J.; Wiebcke, M.; Caro, J. *J. Am. Chem. Soc.* **2009**, *131*, 16000−16001. (c) An, J.; Rosi, N. L. *J. Am. Chem. Soc.* **2010**, *132*, 5578−5579.

(8) (a) Fateeva, A.; Horcajada, P.; Devic, T.; Serre, C.; Marrot, J.; Grenèche, J.-M.; Morcrette, M.; Tarascon, J.-M.; Maurin, G.; Férey, G. *Eur. J. Inorg. Chem.* **2010**, 3789−3794. (b) Brozek, C. K.; Dincă, M. *J. Am. Chem. Soc.* **2013**, *135*, 12886−12891.

(9) (a) Viciu, M. S.; Grasa, G. A.; Nolan, S. P. *Organometallics* **2001**, *20*, 3607−3612. (b) Cucullu, M. E.; Nolan, S. P.; Belderrain, T. R.; Grubbs, R. H. *Organometallics* **1999**, *18*, 1299−1304. (c) Chang, F.; Kim, H.; Lee, B.; Park, H. G.; Park, J. *Bull. Korean Chem. Soc.* **2011**, *32*, 1074−1076.

(10) Persinger, J. D.; Hayes, J. L.; Klein, L. J.; Peters, D. G.; Karty, J. A.; Reilly, J. P. *J. Electroanal. Chem.* **2004**, *568*, 157−165.

(11) Vanalabhpatana, P.; Peters, D. G. *Tetrahedron Lett.* **2003**, *44*, 3245−3247.

(12) Cho, S.-H.; Ma, B.; Nguyen, S. T.; Hupp, J. T.; Albrecht-Schmitt, T. E. *Chem. Commun.* **2006**, 2563−2565.

(13) (a) Selby, H. D.; Roland, B. K.; Zheng, Z. *Acc. Chem. Res.* **2003**, *36*, 933−944. (b) Schoedel, A.; Wojtas, L.; Kelley, S. P.; Rogers, R. D.; Eddaoudi, M.; Zaworotko, M. J. *Angew. Chem., Int. Ed.* **2011**, *50*, 11421−11424. (c) Serre, C.; Millange, F.; Surblé, S.; Férey, G. *Angew. Chem., Int. Ed.* **2004**, *43*, 6286−6289.

(14) (a) Dorofeeva, V. N.; Kolotilov, S. V.; Kiskin, M. A.; Polunin, R. A.; Dobrokhotova, Z. V.; Cador, O.; Golhen, S.; Ouahab, L.; Eremenko, I. L.; Novotortsev, V. M. *Chem.—Eur. J.* **2012**, *18*, 5006−5012. (b) Polunin, R. A.; Kolotilov, S. V.; Kiskin, M. A.; Cador, O.; Golhen, S.; Shvets, O. V.; Ouahab, L.; Dobrokhotova, Z. V.; Ovcharenko, V. I.; Eremenko, I. L.; Novotortsev, V. M.; Pavlishchuk, V. V. *Eur. J. Inorg. Chem.* **2011**, *2011*, 4985−4992. (c) Polunin, R. A.; Kolotilov, S. V.; Kiskin, M. A.; Cador, O.; Mikhalyova, E. A.; Lytvynenko, A. S.; Golhen, S.; Ouahab, L.; Ovcharenko, V. I.; Eremenko, I. L.; Novotortsev, V. M.; Pavlishchuk, V. V. *Eur. J. Inorg. Chem.* **2010**, *2010*, 5055−5057. (d) Polunin, R. A.; Kiskin, M. A.; Cador, O.; Kolotilov, S. V. *Inorg. Chim. Acta* **2012**, *380*, 201−210.

(15) Armstrong, C. M.; Bernhardt, P. V.; Chin, P.; Richardson, D. R. *Eur. J. Inorg. Chem.* **2003**, *2003*, 1145−1156.

(16) Altomare, A.; Burla, M. C.; Camalli, M.; Cascarano, G. L.; Giacovazzo, C.; Guagliardi, A.; Moliterni, A. G.; Polidori, G.; Spagna, R. *J. Appl. Crystallogr.* **1999**, *32*, 115−119.

(17) Sheldrick, G. M. *SHELX-97*; University of Göttingen: Göttingen, Germany, 1997.

(18) Van der Sluis, P.; Spek, A. L. *Acta Crystallogr., Sect. A* **1990**, *46*, 194−201.

(19) Chae, H. K.; Siberio-Pérez, D. Y.; Kim, J.; Go, Y.; Eddaoudi, M.; Matzger, A. J.; O'Keeffe, M.; Yaghi, O. M. *Nature* **2004**, *427*, 523−527.

(20) Kahn, O. *Molecular Magnetism*; Wiley: New York, 1993.

(21) Pavlishchuk, V. V.; Addison, A. W. *Inorg. Chim. Acta* **2000**, *298*, 97−102.

(22) Macrae, C. F.; Bruno, I. J.; Chisholm, J. A.; Edgington, P. R.; McCabe, P.; Pidcock, E.; Rodriguez-Monge, L.; Taylor, R.; Streek, J. v.; Wood, P. A. *J. Appl. Crystallogr.* **2008**, *41*, 466−470.

(23) Spek, A. L. *Acta Crystallogr., Sect. A* **1990**, *46*, c34.

(24) (a) Hu, S.; Zhang, J.-P.; Li, H.-X.; Tong, M.-L.; Chen, X.-M.; Kitagawa, S. *Cryst. Growth Des.* **2007**, *7*, 2286−2289. (b) Pavlishchuk, A. V.; Kolotilov, S. V.; Zeller, M.; Shvets, O. V.; Fritsky, I. O.; Lofland, S. E.; Addison, A. W.; Hunter, A. D. *Eur. J. Inorg. Chem.* **2011**, *2011*, 4826−4836.

(25) Gavrilenko, K. S.; Vértes, A.; Vanko, G.; Kiss, L. F.; Addison, A. W.; Weyhermüller, T.; Pavlishchuk, V. V. *Eur. J. Inorg. Chem.* **2002**, *2002*, 3347−3355.

(26) Lytvynenko, A. S.; Mikhalyova, E. A. *Mjöllnir v.0.3—A Program for Powder Magnetochemical Finite Spin-Coupled Systems' Properties Interpretation Using Full-Matrix Spin-Hamiltonian Solution Method*; Kiev, 2013, https://sites.google.com/site/mjollnirmagn/.

(27) Litvinenko, A. S.; Mikhaleva, E. A.; Kolotilov, S. V.; Pavlishchuk, V. V. *Theor. Exp. Chem.* **2011**, *46*, 422−428.

(28) (a) Ostrovsky, S. M.; Werner, R.; Brown, D. A.; Haase, W. *Chem. Phys. Lett.* **2002**, *353*, 290−294. (b) Mikhalyova, E. A.; Kolotilov, S. V.; Cador, O.; Zeller, M.; Trofimenko, S.; Ouahab, L.; Addison, A. W.; Pavlishchuk, V. V.; Hunter, A. D. *Dalton Trans.* **2012**, *41*, 11319−11329.

(29) Alborés, P.; Rentschler, E. *Dalton Trans.* **2010**, *39*, 5005−5019.

(30) Alborés, P.; Plenk, C.; Rentschler, E. *Inorg. Chem.* **2012**, *51*, 8373−8384.

(31) Nicholson, R. S.; Shain, I. *Anal. Chem.* **1964**, *36*, 706−723.

(32) (a) Nanda, K. K.; Addison, A. W.; Paterson, N.; Sinn, E.; Thompson, L. K.; Sakaguchi, U. *Inorg. Chem.* **1998**, *37*, 1028−1036. (b) Pavlishchuk, V. V.; Kolotilov, S. V.; Addison, A. W.; Prushan, M. J.; Butcher, R. J.; Thompson, L. K. *Inorg. Chem.* **1999**, *38*, 1759−1766.

(33) Bernhardt, P. V.; Mattsson, J.; Richardson, D. R. *Inorg. Chem.* **2006**, *45*, 752−760.

(34) Inzelt, G. *J. Solid State Electrochem.* **2002**, *6*, 265−271.

(35) Tian, A.; Ying, J.; Peng, J.; Sha, J.; Pang, H.; Zhang, P.; Chen, Y.; Zhu, M.; Su, Z. *Cryst. Growth Des.* **2008**, *8*, 3717−3724.
(36) (a) Grygar, T.; Marken, F.; Schröder, U.; Scholz, F. *Collect. Czech. Chem. Commun.* **2002**, *67*, 163−208. (b) Itaya, K.; Uchida, I.; Neff, V. D. *Acc. Chem. Res.* **1986**, *19*, 162−168.
(37) (a) Marken, F.; Cromie, S.; McKee, V. *J. Solid State Electrochem.* **2003**, *7*, 141−146. (b) Doménech, A.; García, H.; Doménech-Carbó, M. T.; Llabrés-i-Xamena, F. *Electrochem. Commun.* **2006**, *8*, 1830−1834. (c) Doménech, A.; García, H.; Doménech-Carbó, M. T.; Llabrés-i-Xamena, F. *J. Phys. Chem. C* **2007**, *111*, 13701−13711.
(38) Catalytic dehalogenation of *n*-C_4H_9I in presence of **2** was not studied because of very low values of catalytic currents detected at catalytic dehalogenation of this halide in solution of **1**. In the case of CH_2Br_2, high noncatalytic current was found in MeCN solution on Pt electrode at E_c (the conditions for examination of catalytic activity of **2** in suspension), which obscured studies of catalytic dehalogenation of this compound.
(39) Koshechko, V. G.; Pokhodenko, V. D. *Russ. Chem. Bull.* **2001**, *50*, 1929−1935.
(40) Andrieux, C. P.; Gallardo, I.; Savéant, J.-M. *J. Am. Chem. Soc.* **1989**, *111*, 1620−1626.
(41) (a) Koshechko, V. G.; Pokhodenko, V. D. *Theor. Exp. Chem.* **1997**, *33*, 230−247. (b) Savéant, J.-M. *Adv. Phys. Org. Chem.* **2000**, *35*, 117−192.
(42) (a) Maithreepala, R. A.; Doong, R.-A. *Environ. Sci. Technol.* **2005**, *39*, 4082−4090. (b) Hoshi, N.; Nozu, D. *Electrochemistry* **2006**, *74*, 593−595. (c) Isse, A. A.; Sandona, G.; Durante, C.; Gennaro, A. *Electrochim. Acta* **2009**, *54*, 3235−3243.
(43) (a) Fritz, H. P.; Kornrumpf, W. *Liebigs Ann. Chem.* **1978**, 1416−1423. (b) Grimshaw, J.; Trocha-Grimshaw, J. *J. Chem. Soc., Perkin Trans. 2* **1975**, 215−218.
(44) (a) Gosden, C.; Kerr, J. B.; Pletcher, D.; Rosas, R. *J. Electroanal. Chem.* **1981**, *117*, 101−107. (b) Gosden, C.; Pletcher, D. *J. Organomet. Chem.* **1980**, *186*, 401−409.
(45) Yang, L.; Kinoshita, S.; Yamada, T.; Kanda, S.; Kitagawa, H.; Tokunaga, M.; Ishimoto, T.; Ogura, T.; Nagumo, R.; Miyamoto, A.; Koyama, M. *Angew. Chem., Int. Ed.* **2010**, *49*, 5348−5351.
(46) (a) Gach, P. C.; Karty, J. A.; Peters, D. G. *J. Electroanal. Chem.* **2008**, *612*, 22−28. (b) Sweeny, B. K.; Peters, D. G. *Electrochem. Commun.* **2001**, *3*, 712−715.
(47) Bernhardt, P. V.; Jones, L. A. *Inorg. Chem.* **1999**, *38*, 5086−5090.